Netw Spat Econ
DOI 10.1007/s11067-014-9252-8

Submission to the DTA2012 Special Issue: A Case for Higher-Order Traffic Flow Models in DTA

Ranju Mohan · Gitakrishnan Ramadurai

Abstract An accurate Dynamic Traffic Assignment (DTA) model should capture real world traffic flow dynamics and predict 'dynamic' travel times. Traditional DTA models used simple traffic flow functions such as exit flow functions, delay functions, point queues, and deterministic physical queue models. Recently, simulation based models apply well accepted traffic flow theoretic models to simulate traffic flow. However, a significant number of papers over the last decade have adopted an approximation of LWR traffic flow model, the cell transmission model, for simulating traffic flow in a DTA model. This paper compares three models, namely, LWR, Payne and Aw-Rascle models for their suitability to be embedded in a DTA model. Model calibration and flow simulation is performed separately using two different speed–density relationships. Results showed the importance of choice of speed-density relationship in traffic flow simulation. Models were used to simulate traffic state at different discretization levels and it was observed that as discretization becomes finer, the models' accuracy increases. Finally, the models were applied to a two node, two link network to analyze their performance in a DTA framework. The higher-order models captured congestion dissipation better than LWR model which consistently underestimates congestion and travel time.

Keywords Dynamic traffic assignment (DTA) · Macroscopic traffic flow models · LWR model · Higher order models · Payne model · Aw-Rascle model

R. Mohan · G. Ramadurai (✉)
Department of Civil Engineering, Indian Institute of Technology, Madras, Chennai-600036, Tamil Nadu, India
e-mail: sasthamgmrm@gmail.com

Gitakrishnan Ramadurai
e-mail: gitakrishnan.ramadurai@gmail.com

Published online: 31 July 2014

1 Introduction

Accuracy of DTA model depends on one of its primary components, the traffic flow model. An accurate DTA model should capture real world traffic flow dynamics and predict 'dynamic' travel times. While microscopic simulation has been shown to replicate traffic flow accurately, its computational burden is still prohibitive for applying them within a DTA framework. Traditional DTA models used simple traffic flow functions such as exit flow functions, delay functions, point queues and deterministic physical queue models. These models restrict the traffic behavior, but have an acceptable computational time. Recently, simulation based models apply well accepted traffic flow theoretic models to simulate traffic flow. A significant number of papers (Lo and Szeto 2002b, Jayakrishnan and Mahmassani 2004, Carey 2006, Balijepalli et al. 2010, Zhong et al. 2012, Carey et al. 2013) have adopted an approximation of LWR traffic flow model, the cell transmission model (CTM), for simulating traffic in a DTA model. Simulation models for DTA appear to be more popular with practitioners than mathematical models since they allow greater flexibility in DTA, particularly in representing flow behavior within links or queues and interaction with neighboring links (Carey 2001). Some remarks on the qualitative and quantitative aspects of the traffic flow simulation results of macroscopic continuum models has been given in Papageorgiou et al. (1990). However the paper does not include any comparison of macroscopic continuum traffic flow models when applying for network level applications. The paper has commented on the limited validation results for higher-order traffic flow models using real traffic data. Also, there exist several higher-order traffic flow models which are developed after the remarks by Papageorgiou (1997) (for example, Aw and Rascle (2000), Zhang (2002), and Jiang et al. (2002)) which address the 'negative speed' critism by Daganzo (1995b). In this paper we compare the simulation results from three widely accepted macroscopic continuum models of traffic flow, namely, LWR (Lighthill and Whitham 1955, Richards 1956) model, Payne (1971) model and Aw and Rascle (2000) model, against the results from a microscopic simulation using calibrated parameter values from the real data. More specifically, the aim of this paper is to compare the performance of higher order models with the first order LWR model for accurate prediction of 'dynamic' travel times and hence the quality of DTA outputs.

Macroscopic models are best suited for network wide applications, where macro characteristics of flow (speed, volume, density, travel time, queue length etc.) are of prime interest. Theory of macroscopic traffic flow is borrowed from Newtonian physics/thermodynamics and is only a coarse approximation of empirical evidence. As pointed out by Papageorgiou (1997), the only accurate physical law available for traffic flow is the conservation law. The first well known macroscopic traffic flow model is the LWR (Lighthill and Whitham 1955, Richards 1956) model and is purely based on the flow conservation equation. But the assumption of steady state, equilibrium traffic flow fails to explain phenomena such as stop-and-go waves and platoon dispersion. Realizing that the traffic flow dynamics and instability is highly related to microscopically inhomogeneous conditions, higher order

models were developed of which (Payne 1971) model aroused considerable interest. The model, based on simple car following rule, incorporates a velocity dynamics equation along with the flow conservation equation. This model explained the spatial and temporal changes in velocity, respectively by means of a relaxation and an anticipation term. Daganzo (1995b) criticized that any higher order model with borrowed terms (relaxation term from kinetic theory of gases and anticipation from viscosity effects in gas dynamics) ignore the anisotropic nature of traffic flow and leads to strange predictions (for example, 'the negative speed of vehicles'- one of the two families of waves in Payne model move faster than the vehicle speed). An argument defending the negative speed was proposed by Papageorgiou (1997) that since macroscopic flow models consider only the average speed of vehicles in the section, the 'negative speed' may be interpreted as an indication that some vehicles move faster than others. However, to rectify the negative speed effect in Payne model, Aw and Rascle (2000) used a pressure term expressed as an increasing function of density in the velocity dynamics equation to account for drivers' anticipation to spatially changing traffic behaviour. This model, termed as Aw-Rascle model, also produces two families of waves, but the speed of both are at most equal to the vehicles' speeds and thus avoids the negative speed of vehicles. Following a different rationale, Zhang (1998), Li and Zhang (2001), and Zhang (2002) also introduced a similar model and more recently, this family of models is referred to as ARZ model (Lebacque et al. 2007). In another research paper, Jiang et al. (2002) addressed the negative speed effect by replacing the anticipation term in Payne model by a speed gradient term (instead of the density gradient in other higher order models) and formulated the Speed Gradient (SG) model. The literatures available in the area of higher order continuum traffic flow models are still vast and this paper is highlighting only few of them.

Motivated by reviewed literature, this paper compares three models, namely, LWR, Payne and Aw-Rascle models, for their suitability to be embedded in a DTA model. For this, models' parameters are calibrated for a highway section using travel time and outflow data from a micro-simulation. The calibrated models are applied to a DTA model on a two-node, two-link network to compare equilibrium flow and travel time values. The aim of this paper is to check the potential benefits of higher order models over LWR model for the realistic representation of traffic flow in a DTA framework.

This paper is organized as follows. Section 2 gives a brief review of literature highlighting few quantitative and qualitative aspects while choosing traffic flow models for DTA. Section 3 outlines the basic equation system of the three models discussed above and the numerical schemes used for traffic flow simulation. Section 4 shows the parameter calibration methods and results for the three models. The models' results for different levels of discretizations, and when applied to a specific traffic situation -lane reduction- are shown as subsections. In Section 5, these models are used for dynamic traffic assignment in a two-node, two-link network and the results are compared. Section 6 draws conclusion from the results obtained on the choice of higher order models in DTA.

2 Choice of Simulation Based Traffic Flow Models in DTA- Quantitative and Qualitative Aspects

Among the macroscopic continuum traffic flow models, except for LWR model, the analytical approaches for solution are complex and numerical schemes are the widely used solution procedure. Since all these models are based on continuum flow theory, the accuracy of traffic dynamics captured by these models depends much on the numerical schemes and the time-space discretization used which are related to the quantitative aspects of models in DTA. Cremer and Papageorgiou (1981) verified through simulation that lowering discretization intervals does not create amplified accuracy in macroscopic traffic flow models, and in fact rising the discretization interval leads to much lower computational effort. However, the choice of time space discretization also depends on the type of the numerical scheme to be used. For macroscopic simulation of traffic, the effects of numerical schemes along with different boundary conditions are pointed out by Helbing and Trieber (1999). A more detailed review on the quantitative aspects of macroscopic traffic flow models can be seen in the paper by Papageorgiou (1997).

The desirable properties of any traffic flow model in DTA include flow conservation, flow propagation, First-In-First-Out (FIFO), causality, and reasonable outflow behaviour (Carey and McCartney 2004, Nie and Zhang 2005, Szeto and Lo 2006). Traffic flow models in general, satisfy all these properties, however, the traffic dynamics and dynamic travel time predictions may vary across these models. In the macroscopic approach of traffic flow modelling, the main disadvantage of LWR model widely reported in literature is the inability to explain the instability (oscillatory phenomena) in traffic. Another disadvantage of the model is the prediction of higher speed values for less dense traffic, which leads to a sharp rear-end for the platoon (Papageorgiou 1997). Again, when there is downstream congestion, all higher order models performs substantially more accurately than simple continuum model (Michalopoulos et al. 1992, Papageorgiou 1997). Cremer and Papageorgiou (1981) have shown that the simple continuum model has standard deviation of modelling error (the error when the model is validated with real data of time mean speed and volume) 50-200 % higher when compared to higher order models. Poor performance of Payne model in some cases of freeway lane drop and on-ramp flow metering has been rectified by Cremer and May AD (1986) and Papageorgiou et al. (1990). Jin and Zhang (2003a) reported that when Payne model is stable, it produces similar results to that by LWR model, however, only the Payne model is able to capture the cluster effect when flow is unstable. Mammar et al. (2009) also reported the superiority of ARZ model over the LWR model in reproducing the real traffic.

Motivated by the reported literature on the advantages of higher order models over the LWR model, Section 4 compares two higher order models (Payne and Aw-Rascle models) with the LWR model based on their performance when applied to a highway mid-block section using simple numerical schemes for solution. The numerical schemes used for simulation is shown in the next section.

3 The Models and Numerical Schemes

The section briefly reviews the three models, namely, LWR, Payne and Aw-Rascle models and their numerical schemes used in this paper for simulating the flow dynamics. Dividing the road stretch into cells of length Δx, the flow dynamics at different time intervals of length Δt can be approximated for different models as shown in the following subsections.

3.1 LWR Model

The model gives the dynamic equations for density through the following equations:

$$\frac{\partial k}{\partial t} + \frac{\partial q}{\partial x} = 0 \tag{1}$$

$$u = u_e(k) \tag{2}$$

$$q = ku \tag{3}$$

Here, *x, t, u, k, q* represents the space, time, speed, density, and flow measures respectively, and $u_e(k)$ is the equilibrium velocity. Equation 1 is the flow conservation equation and can be discretized using Lax-Friedrichs scheme as in Eq. 4.

$$k_i^{j+1} = \frac{1}{2}\left[k_{i+1}^j + k_{i-1}^j\right] - \frac{\Delta t}{2\Delta x}\left[q_{i+1}^j - q_{i-1}^j\right] \tag{4}$$

where k_i^j stands for density at section i at time j, q_i^j is the flow at section i at time j, and Δt and Δx are the time and space interval respectively. Once the density is determined, the speed and flow can be computed using Eqs. 2 and 3.

3.2 Payne Model

Along with the Eqs. 1 and 3 in the LWR model, Payne (1971) proposed a partial differential equation describing the dynamics of the velocity u.

$$\frac{\partial u}{\partial t} + u\frac{\partial u}{\partial x} = \frac{u_e(k) - u}{T} - \frac{c_0^2}{k}\frac{\partial k}{\partial x} \tag{5}$$

The second term in the left hand side (L.H.S) denotes convection which describes changes in the mean velocity due to inflowing and out-flowing vehicles. The first term in the R.H.S. denotes relaxation which describes the tendency of traffic flow to relax to an equilibrium velocity in time T. The last term in the R.H.S is the anticipation term that describes driver's anticipation on spatially changing traffic conditions downstream where ${c_0}^2$ is the anticipation constant. Equation 5 can be discretized using upwind scheme as:

$$u_i^{j+1} = u_i^j - \frac{\Delta t}{\Delta x}u_i^j\left(u_i^j - u_{i-1}^j\right) + \frac{\Delta t}{T}\left(u_e(k_i^j) - u_i^j\right) - c_0^2\frac{\Delta t}{\Delta x}\frac{\left(k_i^j - k_{i-1}^j\right)}{k_i^j} \tag{6}$$

However, the Eq. 6 will not work well for specific traffic situation such as lane reduction (see Section 6) and hence the paper uses the discretization equation by Papageorgiou et al. (1990) which is given as:

$$u_i^{j+1} = u_i^j + \frac{\Delta t}{\Delta x} u_i^j \left(u_{i-1}^j - u_i^j\right) + \frac{\Delta t}{T}\left(u_e(k_i^j) - u_i^j\right) - \frac{\eta}{T}\frac{\Delta t}{\Delta x}\frac{\left(k_{i+1}^j - k_i^j\right)}{k_i^j + \kappa} \quad (7)$$

where η is the kinematic traffic viscosity, $\frac{\eta}{T} = {c_0}^2$ and κ is a tuning coefficient for density values near zero.

3.3 Aw-Rascle Model

Aw and Rascle (2000) modified the velocity dynamics equation by Payne using a convective derivative term of density instead of the spatial derivative of pressure.

$$\frac{\partial u}{\partial t} + \left(u - kp'(k)\right)\frac{\partial u}{\partial x} = \frac{1}{T}\left(u_e(k) - u\right) \quad (8)$$

where $p(k)$ is the traffic pressure expressed as an increasing function of density. i.e. they proved that with a suitable choice of the function $p(k)$, the model will predict more reasonable and realistic result which is lacking in the Payne type models (for example, anisotropy and negative speed of vehicles observed in the latter one). Moreover, the model predicts the instabilities for very light traffic. The functional form of $p(k)$ chosen in the model is as follows:

$$p(k) = k^\gamma \quad (9)$$

where γ is a non negative number ($\gamma > 0$). Substituting the pressure term in Eq. 9 to Eq. 8, the model becomes:

$$\frac{\partial u}{\partial t} + \left(u - \gamma k^\gamma\right)\frac{\partial u}{\partial x} = \frac{1}{T}\left(u_e(k) - u\right) \quad (10)$$

To solve the velocity dynamics equation with relaxation term, the upwind scheme is used as shown in Eq. 11.

$$\begin{aligned} &\text{if } u_i^j < \gamma\left(k_i^j\right)^\gamma \quad u_i^{j+1} = u_i^j - \frac{\Delta t}{\Delta x}\left(u_i^j - \gamma\left(k_i^j\right)^\gamma\right)\left(u_{i+1}^j - u_i^j\right) + \frac{\Delta t}{T}\left(u_e(k_i^j) - u_i^j\right) \\ &\text{if } u_i^j < \gamma\left(k_i^j\right)^\gamma \quad u_i^{j+1} = u_i^j - \frac{\Delta t}{\Delta x}\left(u_i^j - \gamma\left(k_i^j\right)^\gamma\right)\left(u_{i+1}^j - u_i^j\right) + \frac{\Delta t}{T}\left(u_e(k_i^j) - u_i^j\right) \end{aligned} \quad (11)$$

The numerical schemes used are of first order since second order methods can produce oscillations and sometimes non–linear numerical instabilities which might give rise to additional traffic jams that do not corresponds to reality (Helbing and Trieber 1999). The convective and relaxational stability of the above numerical schemes are ensured respectively as $\Delta t = \frac{\Delta x}{u_f}$ and $\Delta t \leq T$ where u_f is the free flow speed of traffic.

Next section shows the calibration of models using data from the microscopic simulation of a hypothetical mid-block section.

4 Calibration of Model Parameters

This section explains the calibration procedure adopted for the three models discussed in the previous sections, and the details of calibration can be seen in Section 4.1. The parameters of the three models are calibrated against the microsimulation result from VISSIM. The microscopic simulation of traffic flow on a 3 lane, 1.8 km highway segment is carried out assuming homogeneous traffic comprising only passenger cars. The parameter values for VISSIM are taken from Virginia Transportation Research Council report (Park and Won 2007). The values, for a 5 mile highway segment located on Interstate Highway 64 in Covington, Virginia, as stated in the report, are shown in Table 1.

The time-space grid used for microsimulation is 10 sec-225 m. Since the paper aims to compare the suitability of the above discussed three models for DTA, major performance measures used for models' calibration were Total System Travel Time (TSTT) and the outflow from the section. The total travel time for few randomly selected number of vehicles to pass the highway segment is computed from the cumulative inflow-outflow curves. For an inflow profile shown in Fig. 1, capacity flow from VISSIM for the selected highway segment is observed to be 4744 veh/hr, when plotted the flow-density diagram (Fig. 2).

Iterative Latin Hypercube Sampling (LHS) method is used for models' calibration by minimizing an error function which is expressed in terms of total system travel time and capacity flow as in Eq. 12.

$$E = \alpha \frac{TT_{VISSIM} - TT_{MODEL}}{TT_{VISSIM}} + (1-\alpha)\frac{Q_{maxVISSIM} - Q_{maxMODEL}}{Q_{maxVISSIM}} \quad (12)$$

Table 1 Calibrated values of VISSIM parameters

VISSIM Parameters	Calibrated Values
Speed limit (mph)	47.5
Minimum headway (front/rear) (m)	0.72
Maximum deceleration (m/sec^2)	−1.04
Average standstill distance, $CC0$ (m)	1.74
Headway at a certain speed, $CC1$ (sec)	2.77
Longitudinal oscillation, $CC2$ (m)	4.09
Start of the deceleration process, $CC3$ (sec)	−0.91
Minimal closing, $CC4$ (m/sec)	−0.97
Minimal opening, $CC5$ (m/sec)	0.86
Speed dependency of oscillations, $CC6$ (10-4 rad/s)	10.7
Oscillations acceleration, $CC7$ (m/sec^2)	0.67
Acceleration behaviour at starting, $CC8$ (m/sec^2)	2.06
Acceleration behaviour near to 80 km/hr speed, $CC9$ (m/sec^2)	2.77

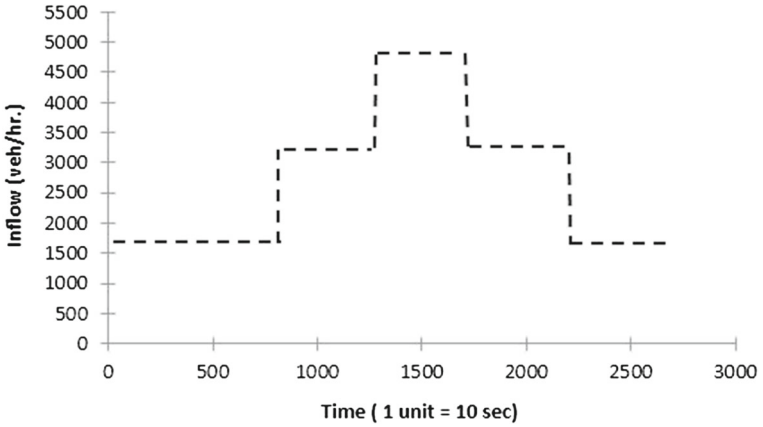

Fig. 1 Inflow profile for simulation

where TT_{VISSIM} and TT_{MODEL} are the total system travel time (for 700 vehicles) from VISSIM and from the model respectively, $Q_{maxVISSIM}$ and $Q_{maxMODEL}$ are the capacity flows in VISSIM and the model respectively, and α_0 is the weightage assumed. The steps followed in the iterative LHS method are as follows:

1. Fix preliminary ranges for each of the model parameters.
2. Generate 'n' different sets of parameters through LHS and compute the error E for each set.
3. Fix new ranges for parameters that give minimum values for the error function, E.
4. Go through steps 2 and 3 iteratively till the parameter range converges.

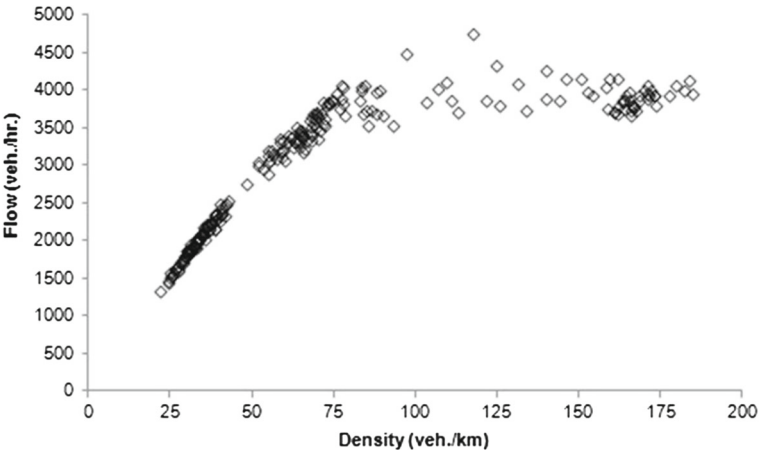

Fig. 2 Flow-density diagram in VISSIM at section x=1

For comparing outflow results Mean Bias Error (MBE) and Coefficient of Variation-Root Mean Square Error (CV-RMSE) are used as shown in Eqs. 13 and 14.

$$MBE\,(\%) = \frac{\sum_t (Outflow_{VISSIM} - Outflow_{MODEL})}{\sum_t Outflow_{VISSIM}} \times 100 \tag{13}$$

$$CV - RMSE = \frac{\sqrt{\left(Outflow_{VISSIM} - Outflow_{MODEL}\right)^2 \times T_s}}{\sum_t Outflow_{VISSIM}} \times 100 \tag{14}$$

Here, $t = 1, 2, ., T_s$ where T_s is the total number of simulation time intervals.

4.1 Importance of Speed-Density (u-k) Relationship on Models' Performance

Equilibrium speed of traffic is one of the key elements in all the four models and hence the speed-density relationship for these models cannot be assumed randomly. In this section, parameter values for the three models are calibrated when using two different u-k relationships. Also, the models' performances are compared when simulating flow dynamics with these different relationships. For first set of simulation, Pipes-Munjal model (Pipes 1967) is used and for the second set, Van-Aerde's model (Rakha and Crowther 2002) is chosen. Model parameters for both the u-k relationship are calibrated separately and are described in the following two sub sections. A time-space discretization of 10 sec-225 m is chosen for the numerical schemes. For the schemes to be stable, the maximum value of free flow speed used is limited to 80 km/hr.

4.1.1 Simulation and Parameter Calibration Using Pipes-Munjal Speed-Density (u-k) Relationship

The speed density relationship assumed is as in Eq. 15.

$$u = u_f \left[1 - \left(\frac{k}{k_j}\right)^a\right] \tag{15}$$

where k_j is the jam density, a is a constant (Pipes-Munjal model assumes integer values for this parameter; however in this section we calibrate this parameter) and u, u_f and k are the speed, free flow speed and density respectively as defined earlier.

The parameters of the three models are calibrated against the microsimulation output from VISSIM (average of 5 runs with different seeds). The inflow profile used for simulation by VISSIM and by the three models are shown in Fig. 3.

During simulation, first 10 minutes are avoided as warm-up period. For the shown inflow profile, the total travel time by VISSIM for 700 vehicles (171^{th} vehicle to 870^{th} vehicle entering the section after warm-up period) is computed as 92545.7 veh-secs with an average travel time of 132.2 secs. The model parameters are calibrated using LHS method as explained in the previous section. Figures 4a and 4b show the result of first two iterations using LHS while calibrating the parameter u_f for LWR model.

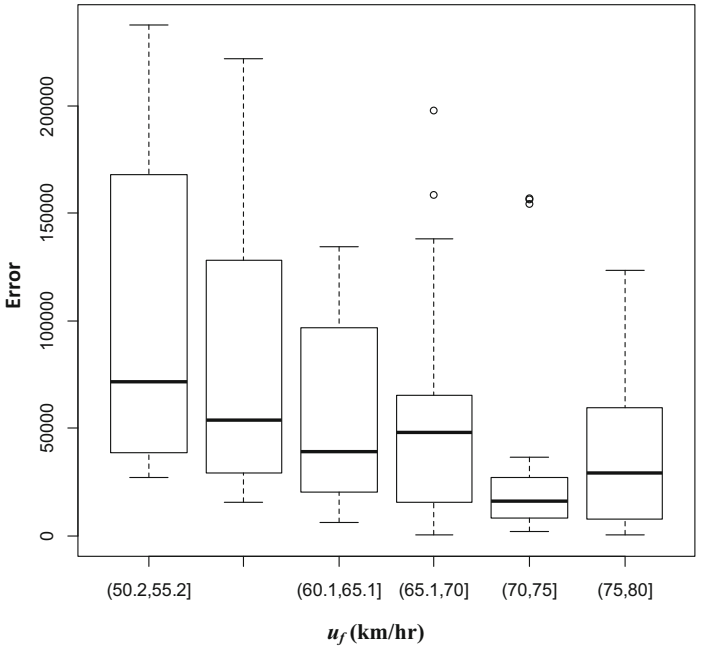

(a) First iteration

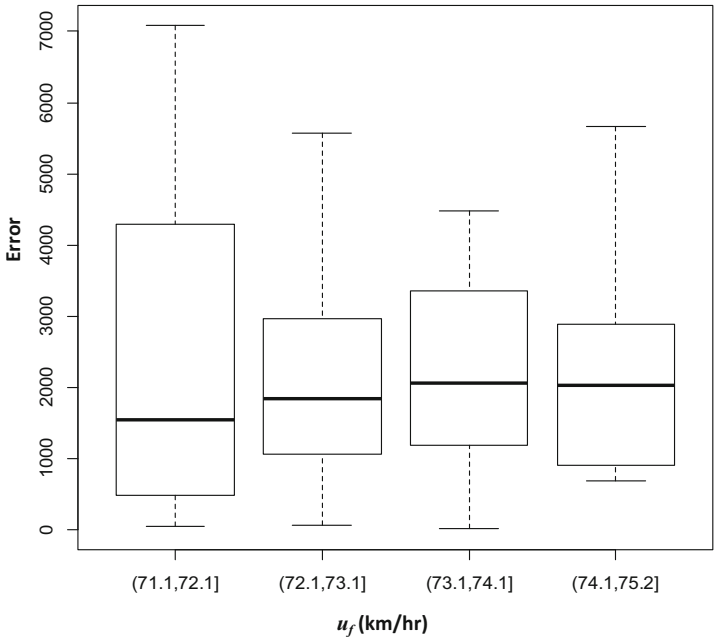

(b) Second iteration

Fig. 3 Calibration of u_f in LWR model

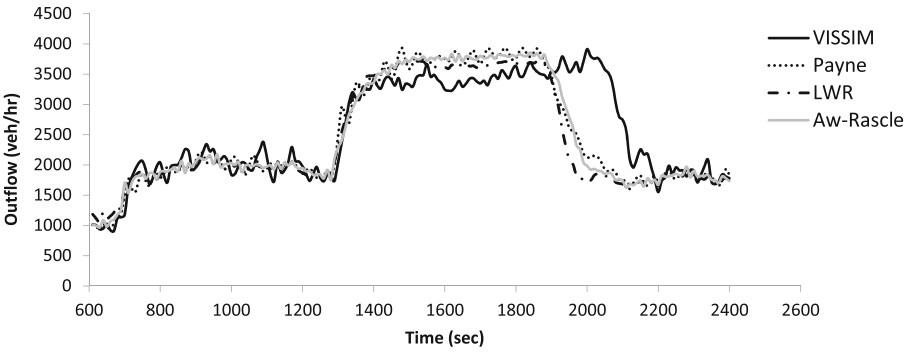

Fig. 4 Outflow from the highway segment over time when using Pipes-Munjal u-k relationship

For the first iteration, 50 km/hr and 80 km/hr are used as minimum and maximum values for LHS sample, which results with a new range of 70-75 km/hr having minimum 'error' and/or error variations as shown in Fig. 4a. The new range is then used as input for the next iteration and the result is shown in Fig. 4b. This iterative sampling continued till the 'error' reduced to a minimum. The parameter values for all the three models are calibrated through a similar procedure and the values are shown in Table 2. All the models seem to give approximately similar results for travel time and error in outflow values (travel time in the range 128-129 sec and MBE in outflow in the range 12.2-12.8 %). The outflow profiles by different models are shown in Fig. 5. With the assumed speed density relationship, congestion dissipation by all the models is found to be in a higher rate than that by the microsimulation. LWR model is dissipating congestion fast, followed by Aw-Rascle and Payne models respectively.

Table 2 Calibrated values of parameters assuming Pipes-Munjal u-k relationship

Parameters		LWR	Payne	Aw-Rascle
u_f (km/hr.)		73.33	63.8	69.77
k_j (km)		276.73	280.27	270.01
η (km^2/hr^2)		–	35.26	–
T (hr.)		–	0.011	0.009
a		1.22	1.08	0.85
κ (veh/km)		–	179.96	–
Average TT (sec)		128	129	129
Outflow	MBE (%)	12.8	12.7	12.3
	$CV-RMSE$	22.4	19.7	20.2

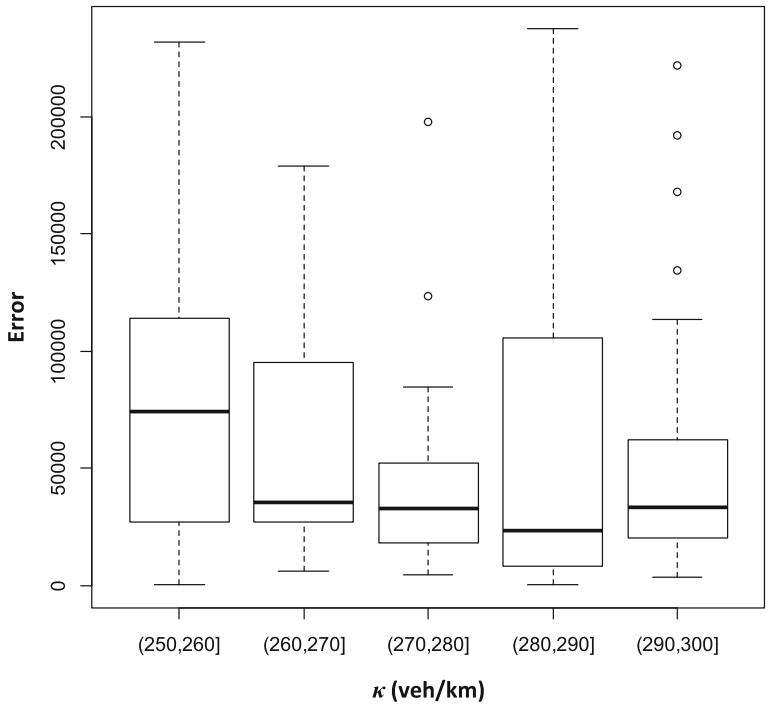

Fig. 5 Calibration of κ in Payne model – first iteration

4.1.2 Simulation and Parameter Calibration Using Van-Aerde's u-k Relationship

Van-Aerde's *u-k* relationship shown in Eq. 16 is a single regime model combining Pipe's car following model and Greenshield's model.

$$k = \frac{1}{c_1 + c_3 u + \frac{c_2}{u_f - u}} \tag{16}$$

where c_1 is the fixed distance headway constant (km), c_2 is the first variable distance headway constant (km^2/hr) and c_3 is the second variable distance headway constant (hr). Model parameters are calibrated with this speed density relationship using the inflow profile shown in Fig. 1. During simulation, first 5 minutes are avoided as warm-up period. For the shown inflow profile, the total travel time by VISSIM for 700 vehicles (171^{th} vehicle to 870^{th} vehicle entering the section after warm-up period) is computed as 85203.7 veh-secs with an average travel time of 121.72 secs. Model' parameters are calibrated using LHS method and a sample result is shown in Fig. 6.

The calibrated values for the three models when using Van-Aerede's *u-k* relationship is given in Table 3 and corresponding outflow profiles are shown in Fig. 7. The results from all the three models follow the same pattern of outflow. In Payne model when compared to the other two models, frequent small fluctuations are observed giving closer result to that by micro-simulation.

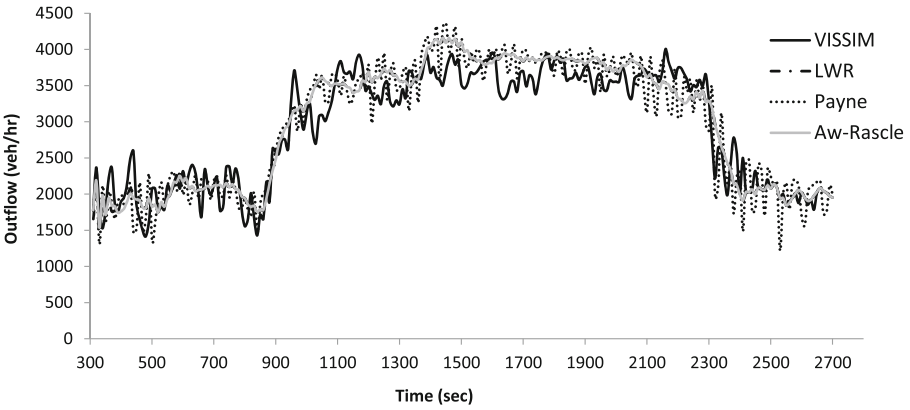

Fig. 6 Outflow from the highway segment over time by Van-Aerede's u-k relationship

To summarize, for each of the speed-density relationship assumed, with the chosen numerical schemes for macroscopic approaches, model performances were similar. Again, from the results of average travel time values and the statistical measures of outflow, Van-Aerde's u-k relationship was found to capture the simulated results more closely than the Pipes-Munjal model. Thus, it is clear, that it is not only the type of model, but also the speed-density relationship that affects the ability to capture the flow dynamics.

4.2 Model Comparison for Different Levels of Discretization

With the chosen numerical schemes and the time space discretization of 10 sec-225 m, the previous section did not provide any major difference in the performance of

Table 3 Calibrated values of parameters assuming Pipes-Munjal u-k relationship

Parameters		LWR	Payne	Aw-Rascle
u_f (km/hr)		54.9	53.97	54.71
c_1 (km)		5.12E-04	1.40E-04	5.35E-04
c_2 (km^2/hr)		5.15E-04	4.18E-04	5.85E-04
c_3 (hr)		1.99E-04	2.07E-04	1.98E-04
η (km^2/hr^2)		-	36.46	-
T (hr)		-	0.012	0.012
γ		-	-	0.69
κ (veh/km)		-	234.35	-
Average TT (sec)		116.58	116.21	116.2
Outflow	MBE (%)	9.94	9.83	9.95
	$CV-RMSE$	12.46	12.53	12.5

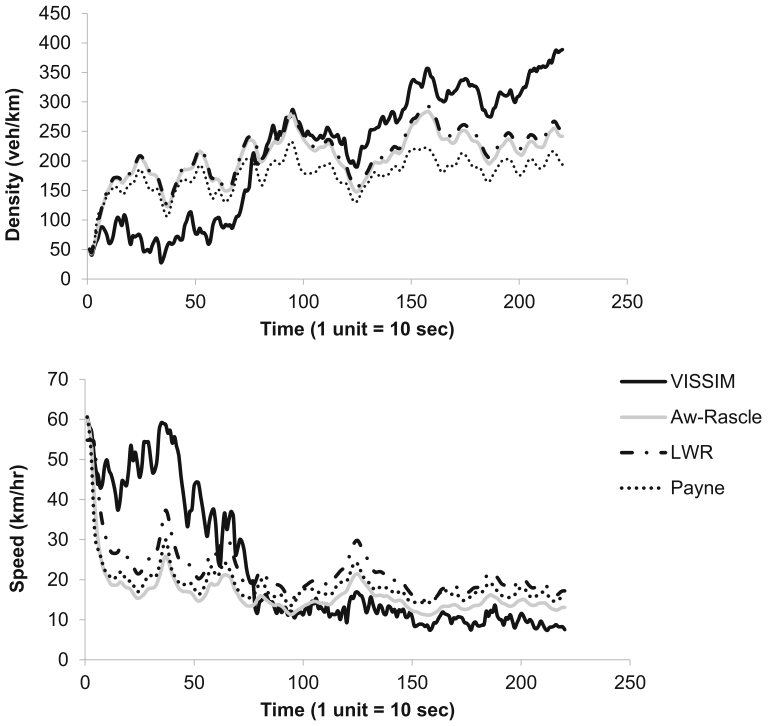

Fig. 7 Density and speed variation over time - before bottleneck

higher order models (Payne and Aw- Rascle models) over the LWR model. Since, models' performance may vary with the time space discretization used, in this section, the results from the three models are compared for three levels of discretization, i.e., 5 sec-112.5m, 10 sec-225 m and 20 sec-450 m. LWR model seems to have higher percentage difference in travel time for all the three discretization levels. Again for LWR model even with finer discretization (5 sec-112.5 m), significant improvement in the result is not observed. The percentage deviations of travel time are found to be in the range of 3.3-6.2 % with lesser value as discretization becomes finer. Result of 20 sec-450 m discretization level is about 2-3 % higher than with 5 sec-112.5 m level (Table 4). Hence, as discretization becomes finer, the accuracy of models' prediction appears to be increasing, but there may exist an optimum discretization level, beyond which further improvement in the results is not possible, and only results in increased computational effort (Papageorgiou et al. 1990).

4.3 Model Performance for Lane Reduction

Instability in traffic can be observed more when there exists specific traffic instances such as lane reduction and traffic signals. In this section, the performances of the models are compared when simulating a lane reduction situation. The three lane road used for parameters calibration is reduced to two lanes at the 4^{th} section

Table 4 Percentage difference in travel time for various discretization levels

Model	% Difference in Travel Time		
	5sec-112.5m	10sec-225 m	20sec-450 m
LWR	4.52	4.56	6.24
Payne	3.49	4.52	6.23
Aw-Rascle	3.35	4.53	5.65

(x = 0.675 km to 0.9 km). Van–Aerde's u-k relationship is assumed for simulation. A constant inflow of 3450 veh/hr is assumed for 220 time intervals (36.67 minutes). Travel times for 1300 vehicles are used to compare the models performance. The results are shown in Table 5.

Payne and Aw-Rascle models produce closer result to that by micro-simulation compared to the LWR model. The speed and density variations before, at, and after bottleneck created by lane reduction are shown in Figs. 8, 9, and 10. Before bottleneck (Fig. 8), a sharp decrease in speed than that by micro-simulation is observed for all the models over the first few minutes of simulation. The speed and density values by VISSIM is by a microscopic simulation and can better capture the traffic state before a bottleneck than by any macroscopic models. For the macroscopic models shown, For the macroscopic models shown, bottleneck activation happens instantaneously, thus speed drops and density rises immediately. During congestion formation, the speed values from LWR were closer to that by the micro-simulation model, but once the flow is congested, LWR model predicts higher speed. At bottleneck, the increase in density and hence decrease in speed was observed in Payne and Aw- Rascle model which are closer to that by micro-simulation compared to the simple continuum model (or LWR model). Just after bottleneck, for LWR model, vehicles were found to have nearly free flow speed, but for other two models speed values were found to be more closer to that by VISSIM. The phenomena of congestion dissipation are captured better in Payne and Aw-Rascle model.

For the results shown in Table 4, Payne model is discretized using Papageorgiou's (1990) scheme. The upwind method for Payne model includes an anticipation constant c_0^2 (parameter c_0 is termed as *traffic sound speed* or *kinematic wave speed*), to which the simulation results are found to be more sensitive. The results for varying c_0 in the upwind scheme of Payne model is shown in Figs. 11 and 12.

Table 5 Models performance for lane reduction

Model	Average Travel Time (sec)	% Difference in Outflow
VISSIM	190.13	
LWR model	158.14	2.97
Payne model	182.02	1.77
Aw-Rascle model	176.49	2.11

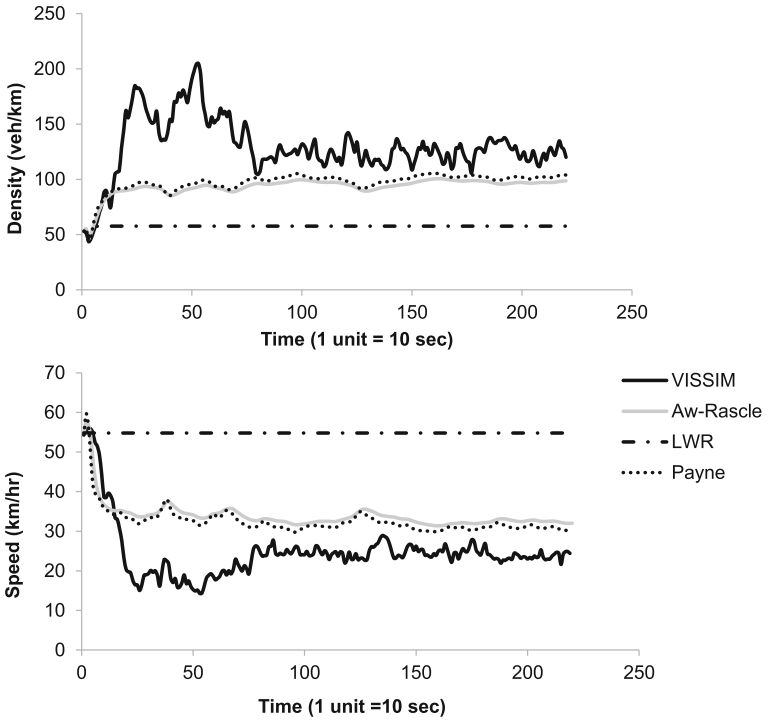

Fig. 8 Density and speed variation over time - at bottleneck

With the calibrated value of 33.29 of this parameter, after 60 sec of simulation time, on the road section before bottleneck, the density suddenly jumps to a high value which leads to negative speed. Reducing the value to 29 km/hr., resolves this unstable behavior before bottleneck, but, at bottleneck, the constant speed achieved differs widely from that in micro-simulation (Fig. 12).

Thus, to improve the performance of Payne model for widely varying density conditions, this paper uses the discretization scheme by Papageorgiou et al. (1990) instead of upwind scheme.

5 Models and Dynamic Traffic Assignment

Sections 3 and 4 highlighted only one of the two prime components of DTA- the traffic flow model. The present section incorporates the traffic flow models in a DTA framework.

Here, the traffic flow models discussed in the previous sections are used to propagate flows on a two node, two link network with fixed O-D (Origin- Destination) demand, and flows are assigned using iterative MSA (Method of Successive Averages) algorithm. Link 1 and Link 2 are of 3 lanes and 1.8 km length and the models' performances are analyzed for two cases:

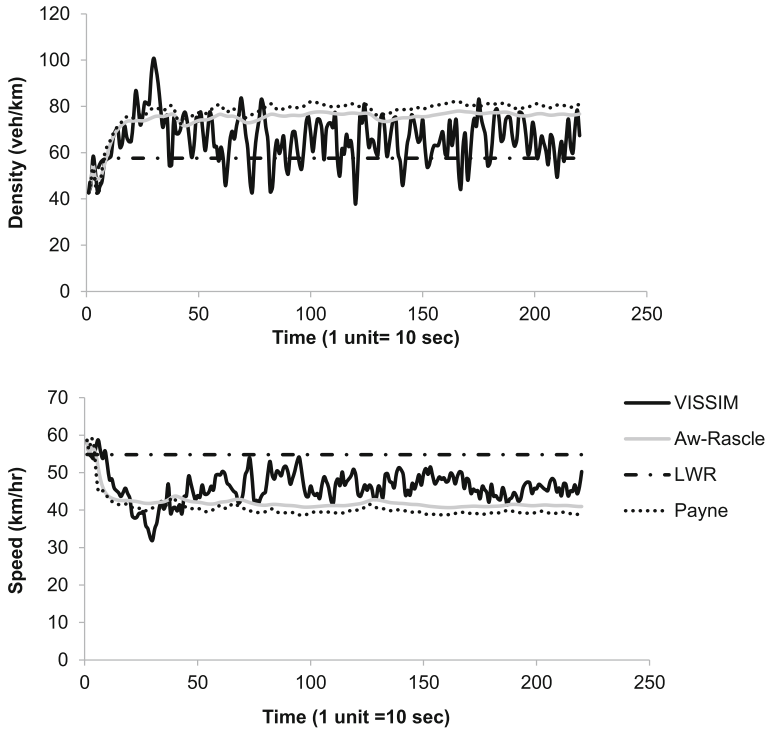

Fig. 9 Density and speed variation over time - after bottleneck

Case (i). Link 2 contains a signal, installed mid-way. Signal cycle length assumed was 120 sec with 50 sec red interval

Case (ii). On link 2, a lane is reduced for 225 m length, after 0.675 km from the origin

A 15 minutes O-D demand as in Fig. 13 is assigned to the network and simulation is performed for 30 minutes. As initial condition, traffic volume on each link is assumed to be zero. The details of the traffic assignment are as follows.

5.1 Dynamic User Equilibrium (DUE) and Traffic Assignment

The commonly adopted route choice principle is the dynamic extension of Wardrop's (Wardrop 1952) principle, called the Dynamic User Equilibrium (DUE) which can be defined as follows: 'At each instant of time, from each origin to destination, the travel time that travelers experience on any used routes are equal and minimal and less than or equal to the minimum travel time on any unused route'. The solution approach used for solving dynamic network equilibrium problem is based on a temporal discretization into periods τ=1,2,....,$\left|\frac{T_d}{\Delta t}\right|$ where Δt is the chosen duration of a departure time interval and T_d is the total time period of assignment (Florian et al. 2005). If l denotes the path, the time varying demands and path flows are denoted by

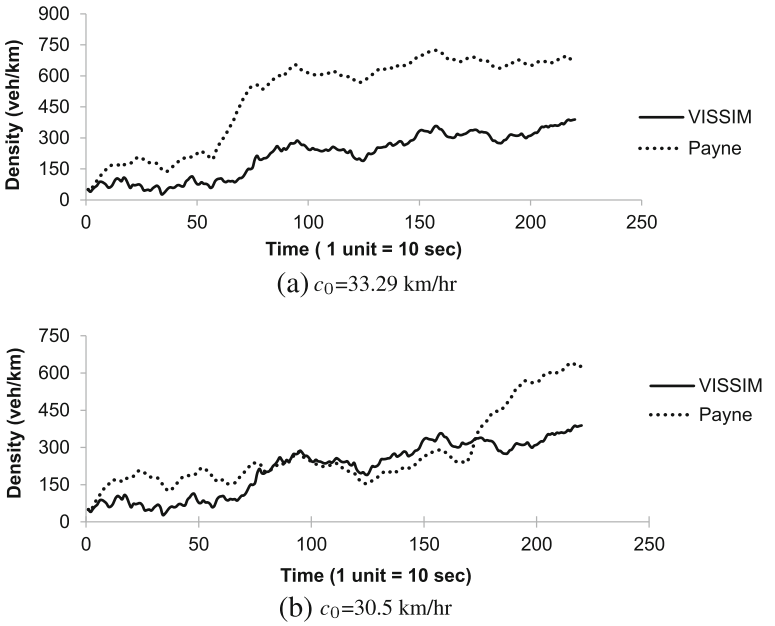

Fig. 10 Density variation before bottleneck in Payne model when using upwind scheme

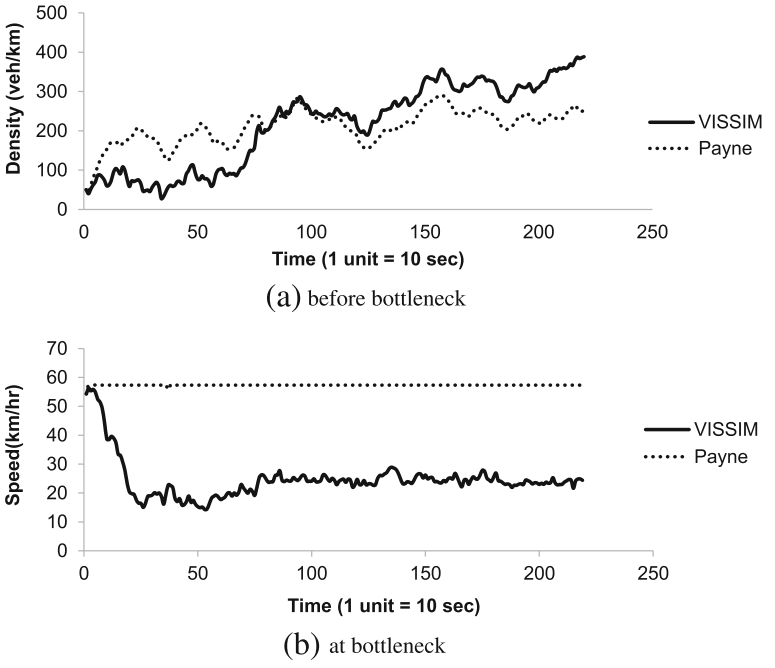

Fig. 11 Density and speed variation in Payne model for c_0=29.0km/hr

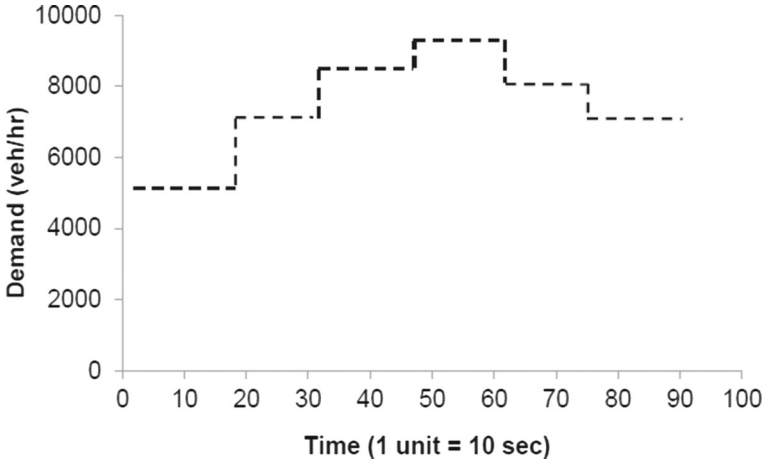

Fig. 12 Fixed O-D demand profile to the network

$g(\tau)$ and $h_l(\tau)$ respectively. The path flow rates in the feasible region Ω satisfy the conservation of flow and non-negativity constraints as:

$$\Omega^{\tau} = \left\{ h(\tau) : \sum_{l} h_l(\tau) = g(\tau);\ \forall\tau,\ h_l(\tau) \geq 0;\ \forall l,\ \forall\tau \right\} \tag{17}$$

DUE can be expressed using a temporal version of Wardrop's (1952) user optimal route choice definition as:

$$\left.\begin{array}{ll} s_l(\tau) = u(\tau) & \text{if } h_l(\tau) > 0 \\ s_l(\tau) \geq u(\tau) & \text{otherwise} \end{array}\right\} \forall l,\ \forall\tau \tag{18}$$

where $u(\tau) = \min_{l}\{s_l(\tau)\}$ and $s_l(\tau)$ is the path travel time. To reach the above DUE solution, an iterative MSA algorithm by Florian et al. (2005) is used for flow assignment to each path (for the sample network used in the paper path flow equals link flow). The three traffic flow models (LWR, Payne, and Aw-Rascle models) are embedded into the MSA algorithm and outflow from the links are determined through discrete time simulation. The link (path) travel times are determined using the cumulative inflow-cumulative outflow values (Ramadurai and Ukkusurai 2010, Lo and Szeto 2002a). The algorithm is summarized below.

5.1.1 Algorithm

- Step 0:Initialization (Iteration counter n=1).
  - Assign flows to each link equally

$$h_1(\tau) = h_2(\tau) = \frac{g(\tau)}{2};\ \forall\tau$$

- Step 1: Traffic flow propagation

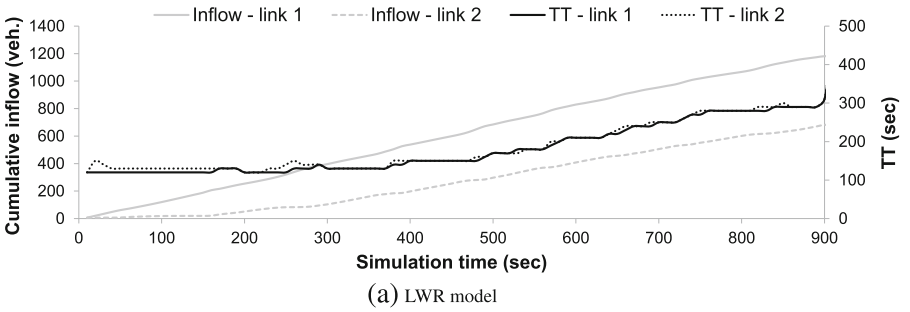

(a) LWR model

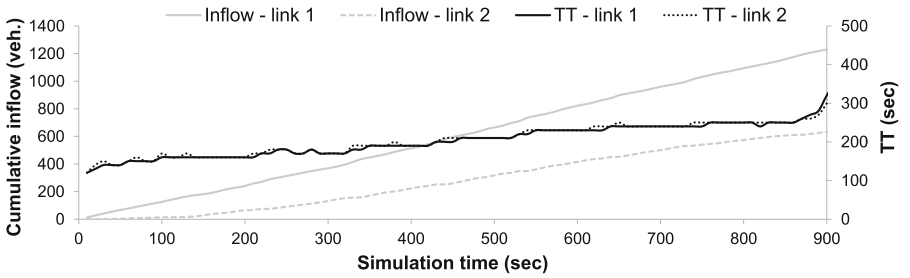

(b) Payne model

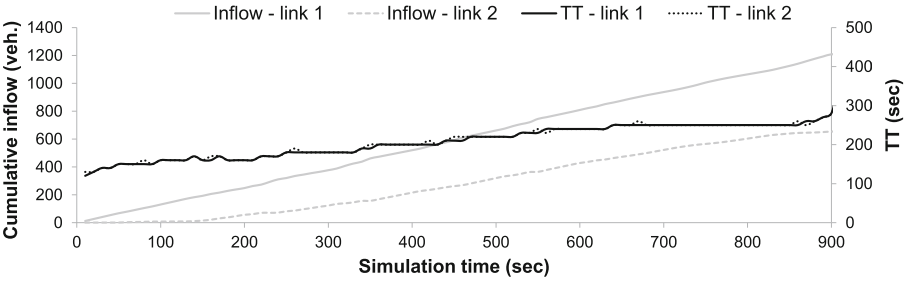

(c) Aw-Rascle model

Fig. 13 Demand and travel time variation for links 1 and 2 for Case (i)

- Step 1a: Calculate initial state (τ=1) of link l ($l = 1, 2$)
  - At section $i = 0$, $q_i^\tau(l) = h_l(\tau)$ (Inflow to link l)
  - Assuming equilibrium speed $u_e(k_0^\tau)$ for section i=0, find density k_0^τ
  - $\forall i \neq 0$ assume negligible densities and free flow speed
- Step 1b: $\forall l,\ \forall i,$ and $\tau = 2 \ldots \frac{T_d}{\Delta t}$
  - Simulate density ($k_i^\tau(l)$) for all traffic flow models using Eq. 4 and speed ($u_i^\tau(l)$) for Payne or Aw-Rascle models using Eqs. 7 and 11

  - ∗ At section $i = \frac{L}{\Delta x}$, $q_i^\tau(l) = k_i^\tau(l) u_i^\tau(l)$ (Outflow form link l) where $u_i^\tau(l) = u_e\left(k_i^\tau(l)\right)$ for LWR model
  - ∗ Cumulative inflow to link l at time τ : $Q_{in}(l,\tau) = Q_{in}(l,\tau-1) + q_0^\tau(l)$
  - ∗ Cumulative outflow to link l at time τ : $Q_{out}(l,\tau) = Q_{out}(l,\tau-1) + q_i^\tau(l)$ where $i = \frac{L}{\Delta x}$

- Step 2: Travel time computation
  - $\forall l$ and $\forall \tau$, compute travel time using cumulative inflow-outflow values
- Step 3: Reallocation of input demands to paths/links
  - Identify the shortest among the used paths/links. Redistribute the flow as follows.

$$h_l^n(\tau) = \begin{cases} h_l^{n-1}(\tau)\frac{n-1}{n} + \frac{g(\tau)}{n}, & \text{if } s_l^n(\tau) = u^n(\tau) \\ h_l^{n-1}(\tau)\frac{n-1}{n}, & \text{otherwise} \end{cases} ; \ \forall \tau, \forall l \quad (19)$$

- Step 4: Stopping rule:
  - $n = n + 1$
  - If $n > N$ (N is some pre-specified number of iterations) or *Relative Gap (n)*$\leq \epsilon$, STOP, otherwise go to step 1. *Relative Gap* (n) is given by

$$\textit{Relative gap} \ \ (n) = \max_\tau \left(\frac{\sum_l s_l^n(\tau) h_l^n(\tau) - u^n(\tau) g(\tau)}{u^n(\tau) g(\tau)} \right)$$

5.2 Discussion of Results for Case (i) and Case (ii)

Figures 14 through 15 show the cumulative equilibrium inflows for link 1 and link 2 (Inflow-link 1 and Inflow-link 2) and the corresponding travel times (TT-link 1 and TT-link 2) respectively for LWR, Payne and Aw-Rascle models for Case (i) and Case (ii).

For Case (i), where the link 2 contains a signal, the delay experienced by the vehicles on this link is expected to be higher than for the vehicles on link 1. For the first 70 sec of simulation, signal was green, then changes to red for the next 50 sec, and likewise operates alternatively till the end of simulation time. In the first 150 sec of simulation, since the traffic demand was low, LWR predicts Free Flow Travel Time (FFTT) on link 1 and slightly higher travel time on link 2 because of the signal, whereas, for the same period, higher order model predicts a step by step increase of TT. The travel times predicted by all the three models are increasing because of the peak demands between 300^{th} to 750^{th} second. From all models, travel times on both links are found to be almost equal and it is observed that DUE is achieved comparatively well in Aw-Rascle model, followed by Payne and LWR models.

In Case (ii), there is a bottleneck on link 2 because of lane reduction. Behaviour of models for lane reduction has been discussed in Section 4 earlier where LWR model seemed to under predict congestion. From Figs. 14a, b and c, it can be seen

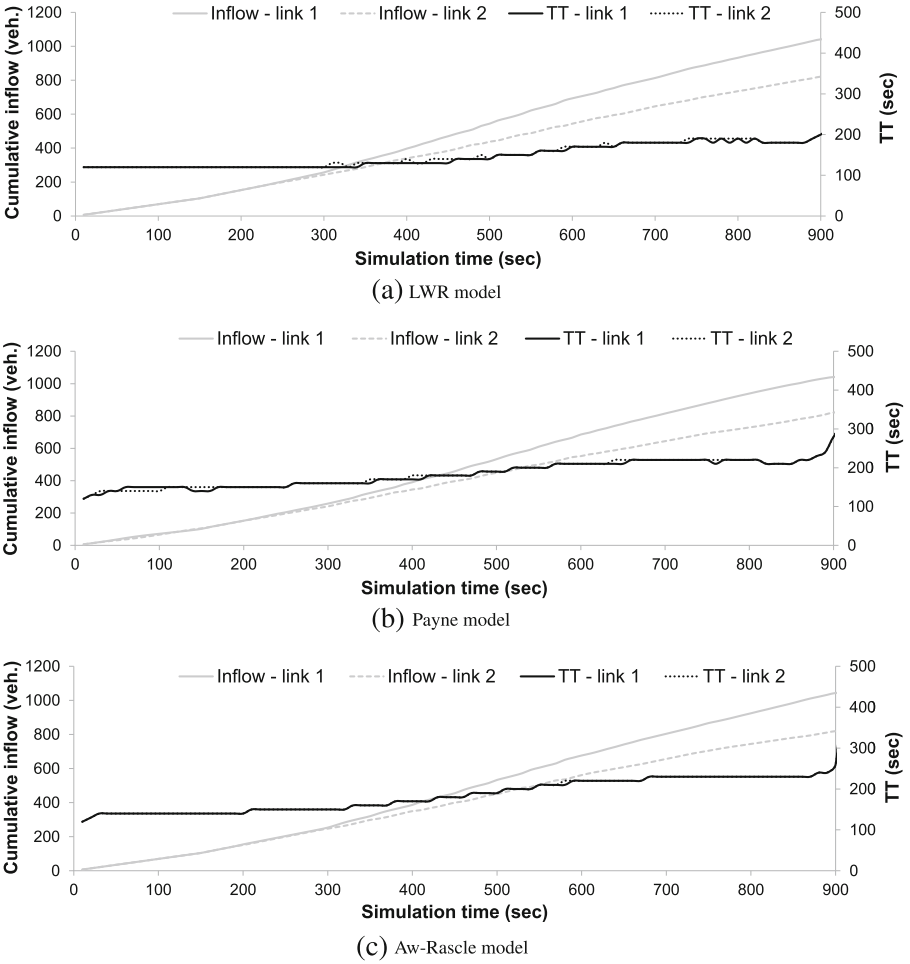

(a) LWR model

(b) Payne model

(c) Aw-Rascle model

Fig. 14 Demand and travel time variation for links 1 and 2 for Case (ii)

that DUE condition is better achieved in Aw- Rascle model, followed by LWR model and Payne model, but the link travel times are less in LWR model compared to the other two models.

TSTT values and cumulative inflows to links from the models are shown in Table 6. For Case (i), equilibrium flow values to link 1 and link 2 predicted by each models are different; but, for Case (ii) flows by different models are almost equal. However, for both cases LWR model gives lesser TSTT compared to the higher order models, thus under predicting congestion.

To summarize, compared with the LWR model, higher order models are better capturing the congestion dissipation in the link with signals or having lane reduction, thereby resulting in a different dynamic user equilibrium solution. LWR model appear to under predict the time required for congestion to clear while the two higher

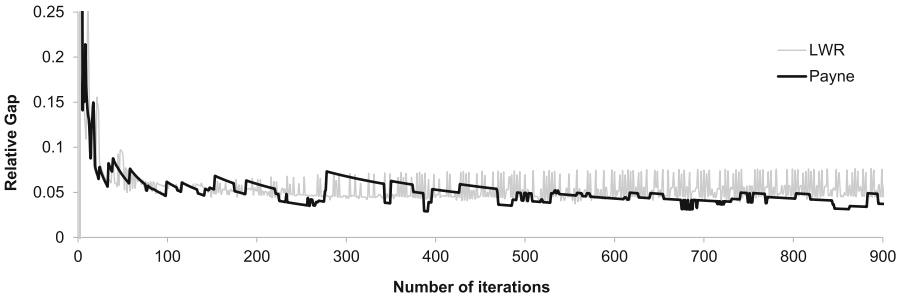

(a) LWR and Payne models

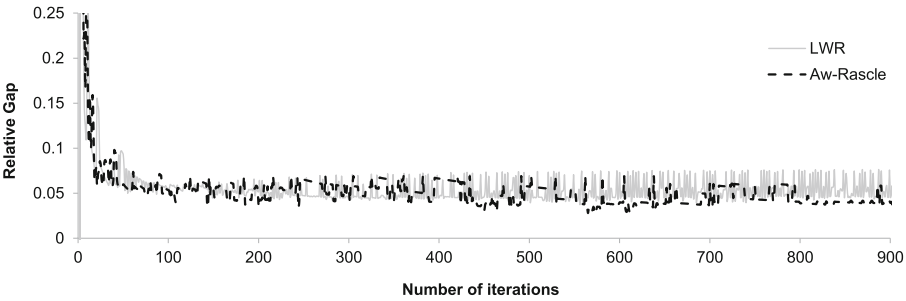

(b) LWR and Aw-Rascle models

Fig. 15 Comparison of convergence

order models – Payne and Aw-Rascle are better capturing congestion dissipation perhaps due to their ability to model stop-and-go waves in congested traffic.

5.3 Defining Quality of the Models' Outputs

In this section, the quality of the DTA model based on the three traffic flow models is described from two dimensions: convergence and realism of traffic dynamics (these two aspects are highlighted in *A primer for dynamic traffic assignment*, (ADB30 Transportation Network Modelling Committee 2010)). The realism of traffic dynamics by different models has been analyzed in Section 4. The present section shows

Table 6 TSTT and Cumulative inflow to links at DUE

Model	Case (i)			Case (ii)		
	Cumulative Inflow (veh)		TSTT (veh-min)	Cumulative Inflow (veh)		TSTT (veh-min)
	Link 1	Link 2		Link 1	Link 2	
LWR	1181.34	681.16	5711.53	1041.19	821.31	4594.37
Payne	1229.04	633.46	6454.83	1040.8	821.69	5774.54
Aw-Rascle	1208.71	653.78	6600.64	1043.28	819.21	5839.21

the convergence of the DTA algorithm while using these different traffic flow models. The measure used for the convergence check is the relative gap and a graph showing the iterative response of relative gap is plotted as in Fig. 15. Minimum relative gap achieved by the LWR model is around 0.05, oscillating between 0.05 to 0.075, whereas Payne and Aw-Rascle models find a better solution beyond 0.05. Payne model is observed to have better convergence than Aw-Rascle model, followed by LWR model. LWR model has frequent spikes and oscillation as seen in the figure.

6 Conclusion

Accuracy of any DTA model depends mainly on its ability to predict dynamic travel times which in turn is related to the reproduction of realistic traffic phenomena. Superiority of higher order models over simple LWR model in simulating traffic flow have been discussed in past decades and this paper compared two higher order models, namely, Payne and Aw-Rascle model, with the LWR model for embedding in a DTA framework.

Model calibration and flow simulation is performed separately using two different speed–density relationships. Results showed the importance of the choice of speed-density relationship in traffic flow simulation. Models were used to simulate traffic state at different discretization levels and it was observed that as discretization becomes finer, the models' accuracy is increased. Higher order models are observed to have minimum percentage difference in outflow when compared to the LWR model. Again, for testing the models' performances in a congested traffic instance, flows were simulated for a bottleneck section with the calibrated macroscopic traffic flow models and compared with data from a VISSIM micro-simulation. Payne and Aw-Rascle models gave closer results to VISSIM and LWR model seemed to produce widely varying result while dissipating congestion.

Finally, the models were applied to a two node, two link network to analyze their performance in a DTA framework. DUE solutions for two cases – a) when one of the link is signalized, and b) when there is a lane reduction in one link – are compared for the three models. All the three models were observed to be giving dynamic user equilibrium flow for both the cases. However, Payne and Aw-Rascle were better at capturing the congestion dissipation in the link with signals thereby resulting in a different dynamic user equilibrium solution. In both the cases, Aw-Rascle model is observed to have comparatively well-defined DUE solution followed by Payne and LWR models. From the TSTT predicted by the three models, it can be concluded that the choice of traffic flow models could result in different results in a DTA model, with higher order models providing more reasonable results compared to LWR model, especially when considering congested conditions. While checking the quality of DTA models output, it is observed that the Payne model shows better convergence to DUE solution followed by Aw-Rascle and LWR model respectively.

There exist several avenues for improvement of the current work. One of the limitations of this work is the absence of real traffic data for calibration and comparison of models. Also, the numerical schemes used for solution will definitely have a major

role in the flow parameter predictions. While the current results indicate a clear benefit of higher order models, calibrating the models with real data, testing alternative numerical schemes, and also testing models' applicability to a larger network are essential future work directions before the case for higher order models can be conclusively judged.

Acknowledgments The authors thank the Ministry of Urban Development, Government of India, for sponsoring the Center of Excellence in Urban Transport at Indian Institute of Technology (IIT), Madras that enabled this research work. The second author also thanks the New Faculty Grant provided by IIT Madras that partially funded this research work. All findings and opinions in the paper are the authors and does not necessarily reflect the views of the funding agencies.

References

ADB30 Transportation Network Modelling Committee (2010) A primer for Dynamic Traffic Assignment. accessed on 2nd June 2012. http://onlinepubs.trb.org/onlinepubs/circulars/ec153.pdf

Aw A, Rascle M (2000) Resurrection of second order models of traffic flow. SIAM J Appl Math 60(3):916–938

Balijepalli C, Carey M, Walting D (2010) Introducing lanes and lane-changing in a cell transmistran model, In: Presented at the third international symposium on dynamic traffic assignment

Carey M (2001) Dynamic traffic assignment with more flexible modelling within links. Netw Spatial Econ 1:349–375

Carey M (2006) Introducing lane-changing into the CTM and DTA. Presentation at UCL traffic flow workshop. http://2222.cege.ucl.ac.uk/cts/TrafficFlow/pdfs/Carey.pdf

Carey M, McCartney M (2004) An exit–flow model used in dynamic traffic assignment. Comput Oper Res 31:1583–1602

Carey M, Balijepalli C, Watling D (2013) Extending the cell transmission model to multiple lanes and lane-changing. Netw Spatial Econ 15:1–29

Cremer M, May AD (1986) An extended traffic flow model for inner urban freeways. In: 5th IFAC/IFIP/IFORS International conference on control in transportation systems, Vienna, pp. 383–388

Cremer M, Papageorgiou M (1981) Parameter identification for a traffic flow model. Automatica 17(6):837–843

Daganzo CF (1995b) Requiem of second-order fluid approximations of traffic flow. Transp Res: Part B 2(4):277–286

Florian M, Mahut M, Tremblay N (2005) Simulation approaches in transportation analysis, Operations research/computer science interfaces series, vol 31. Springer, US

Helbing D, Trieber M (1999) Numerical simulation of macroscopic traffic equations. Comput Sci Eng 1(5):89–98

Jayakrishnan R, Mahmassani HS (2004) An evaluation tool for advanced traffic information and management systems in urban networks. Transp Res: Part C 2(3):129–147

Jiang R, Wu QS, Zhu ZJ (2002) A new continuum model for traffic flow and numerical tests. Transp Res: Part B 36:405–419

Jin WL, Zhang HM (2003a) The formation and structure of vehicle clusters in the payne-whitham traffic flow model. Transp Res: Part B 37:207–223

Lebacque JP, Mammar S, Haj-Salem H (2007) The aw-rascle and zhang's model: Vacuum problems, existence and regularities of the solutions of the riemann problem. Transp Res: Part B 41:710–721

Li T, Zhang HM (2001) The mathematical theory of an enhanced nonequilibrium traffic flow model. Netw Spatial Econ 1:167–177

Lighthill MJ, Whitham GB (1955) On kinematic waves. ii, a theory of traffic flow on long crowed roads. Proc Roy Soc A 229:281–345

Lo H, Szeto WY (2002a) A cell-based variational inequality formulation of the dynamic user optimal assignment problem. Transp Res: Part B 36:421–443

Lo HK, Szeto WY (2002b) A cell–based dynamic traffic assignment model: Formulation and properties. Math Comput Model 35(7-8):849–865

Mammar S, Lebacque JP, Haj-Salem H (2009) Riemann problem resolution and godunov scheme for the aw- rascle-zhang model. Transp Sci 43(4):531–545

Michalopoulos PG, Yi P, Lyrintzis AS (1992) Continuum modelling of traffic dynamics on congested freeways. Transp Res: Part B 27:315–332

Nie X, Zhang MH (2005) A comparitive study of some macroscopic link models used in dynamic traffic assignement. Netw Spatial Econ 5:89–115

Papageorgiou M (1997) Some remarks on macroscopic traffic flow modelling. Transp Res: Part A 32(5):323–329

Papageorgiou M, Blosseville JM, Haj-Salem H (1990) Modelling and real-time control of traffic flow on the southern part of boulevard peripherique in Paris part i: modelling. Transp Res: Part A 24(5):345–359

Park B, Won J (2007) Microscopic simulation models calibration and validation handbook. Tech Rep (VRTC) -07-CR6, Virginia Transportation Research Council

Payne HJ (1971) Mathematical models of public systems. Society for Computer Simulation (Simulation Councils Incorporated)

Pipes LA (1967) Car following models and the fundamental diagram of road traffic. Transp Res 1:21–29

Rakha H, Crowther B (2002) Comparison of greenshields, pipes and van aerde car-following and traffic stream models. Transp Res Rec 1802:248–262

Ramadurai G, Ukkusurai S (2010) Dynamic user equilibrium model for combined activity-travel choices using activity-travel supernetwork representation. Netw Spatial Econ 10:273–292

Richards PI (1956) Shockwaves on the highway. Oper Res 4(1):42–51

Szeto WY, Lo HK (2006) Dynamic traffic assignment: Properties and extensions. Transportmetrica 2(1):31–52

Wardrop JG (1952) Some theoretical aspects of road traffic research. Proceedings of the Institute of Civil Engineers Part, vol II, pp 325–378

Zhang HM (1998) A theory of non–equilibrium traffic flow. Transp Res: Part B 32(7):485–498

Zhang HM (2002) A non-equilibrium traffic model devoid of gas-like behavior. Transp Res: Part B 36(3):275–290

Zhong R, Sumalee A, Panl T, WHK L (2012) A cell transmission model with lane changing and incorporation of stochastic demand and supply uncertainties for freeway traffic state estimation. In: Presented at the Fourth International Symposium on Dynamic Traffic Assignment